FEBS 25263 FEBS Letters 505 (2001) 431–435

Investigating the conformational coupling between the transmembrane and cytoplasmic domains of a single-spanning membrane protein

A ^{1}H-NMR study

Florence Mousson[a], Veronica Beswick[a,1], Yves-Marie Coïc[b], Tam Huynh-Dinh[b], Alain Sanson[a,2], Jean-Michel Neumann[a,*]

[a] *Biophysique des Protéines et des Membranes, CEA DSV/DBCM and URA CNRS 2096, Centre d'Etudes de Saclay, 91191 Gif sur Yvette Cedex, France*
[b] *Unité de Chimie Organique, URA CNRS 487, Institut Pasteur, 28 rue du Dr Roux, 75724 Paris, France*

Received 31 July 2001; revised 21 August 2001; accepted 22 August 2001

First published online 6 September 2001

Edited by Maurice Montal

Abstract PMP1 is a 38-residue single-spanning membrane protein whose C-terminal cytoplasmic domain, Y25–F38, is highly positively charged. The conformational coupling between the transmembrane span and the cytoplasmic domain of PMP1 was investigated from ^{1}H-nuclear magnetic resonance data of two synthetic fragments: F9–F38, i.e. 80% of the whole sequence, and Y25–F38, the isolated cytoplasmic domain. Highly disordered in aqueous solution, the Y25–F38 peptide adopts a well-defined conformation in the presence of dodecylphosphocholine micelles. Compared with the long PMP1 fragment, this structure exhibits both native and non-native elements. Our results make it possible to assess the influence of a hydrophobic anchor on the intrinsic conformational propensity of a cytoplasmic domain.

Key words: Single-spanning membrane protein; Nuclear magnetic resonance; Dodecylphosphocholine micelle

1. Introduction

The interaction network governing the structural properties of membrane proteins takes place in three different environments, i.e. the aqueous phase, the hydrophobic core of the bilayer and the interface milieu. The latter region, highly heterogeneous in terms of both structure and dynamics, exhibits singular physico-chemical properties that increase the difficulty of understanding the molecular mechanisms underlying the membrane protein folding [1,2]. In particular, little is known about the role and extent of conformational coupling between the transmembrane spans and the cytoplasmic/extracellular domains of membrane proteins.

To address these questions, it is necessary to get information at the amino acid level of membrane proteins. An appropriate method consists of studying by nuclear magnetic resonance (NMR) small membrane proteins or fragments solubilized in membrane-mimicking environments, especially that provides by dodecylphosphocholine (DPC) micelles because of the presence of phosphocholine head groups [3–7]. Using this methodology, we have recently undertaken the analysis of the conformational features and lipid-binding properties of the single-spanning membrane protein PMP1, a regulatory subunit of the yeast H^+-ATPase [8,9]. Its C-terminal cytoplasmic domain, corresponding to bold residues in the sequence given below, is highly positively charged: L_1-P-G-G-V_5-I-L-V-F-I_{10}-L-V-G-L-A_{15}-C-I-A-I-I_{20}-A-T-I-I-**Y_{25}-R-K-W-Q-A_{30}-R-Q-R-G-L_{35}-Q-R-F_{38}**

^{1}H-NMR experiments have shown that the PMP1 fragment A18–F38, solubilized in perdeuterated DPC micelles, adopts a single helix conformation from the N-terminus up to Q32 [10]. The N-terminal helix thus includes the truncated hydrophobic segment A18–I24 and a part of the charged cytoplasmic domain, Y25–Q32. The C-terminal extremity, R33–F38, folds back toward the micelle interior [11]. As a result, the PMP1 fragment A18–F38 exhibits a ring-like interfacial distribution of five basic side chains and has been shown by ^{2}H-NMR to specifically bind POPS when inserted in mixed POPC/POPS bilayers [12].

The involvement of both the hydrophobic span and the cytoplasmic domain within the same secondary structure led us to consider PMP1 as a suitable model for investigating the conformational coupling evoked above. With this view, we have analyzed the conformational properties of two synthetic peptides representing two extreme fragments of the PMP1 protein: (i) F9–F38, corresponding to 80% of the whole PMP1 sequence (underlined residues in the aforementioned sequence), and (ii) Y25–F38, corresponding to the isolated PMP1 cytoplasmic domain (bold residues).

2. Materials and methods

2.1. PMP1 fragment synthesis

Peptides were synthesized by using continuous-flow Fmoc/tBu chemistry [13–15] on a Applied Biosystems (Foster City, CA, USA) Pioneer peptide synthesizer. All chemical reagents were purchased

*Corresponding author. Fax: (33)-1-69 08 81 39.
E-mail address: neumann@dsvidf.cea.fr (J.-M. Neumann).

[1] Also from Université d'Evry, Bd. F. Mitterrand, 91025 Evry, France.
[2] Also from Université P.&M. Curie, 9 quai Saint-Bernard, Bât C, 75005 Paris, France.

Abbreviations: DPC, dodecylphosphocholine; NOESY, nuclear Overhauser enhancement spectroscopy; TOCSY, total correlated spectroscopy

0014-5793/01/$20.00
PII: S0014-5793(01)02864-2

from Applied Biosystems. HATU and DIPEA were used as coupling reagents. Peptides were blocked at the N-terminus with an acetyl group and at the C-terminus with an amide. The syntheses were performed using 0.1 mmol of Fmoc-PAL-PEG-PS resin. N-terminal acetylation was achieved on the peptide resin at the end of the synthesis with acetic anhydride.

2.1.1. Fragment 25–38. Stepwise elongation of the peptide chain was done using the extended coupling protocol (yield 97%). A TFA/TIS/thioanisole/water/phenol/EDT 83.5:2.5:2.5:4:5:2.5 (v/v) mixture was used for cleavage. After removal from the resin and deprotection, the cleavage product was precipitated in cold diethyl ether, filtered, dissolved with aqueous trifluoroacetic acid (TFA) buffer and lyophilized (190 mg, yield 99%). Crude peptide was directly purified by reverse-phase medium-pressure liquid chromatography on a Nucleoprep 20 μm C18 100 Å preparative column, using a 0–50% linear gradient of acetonitrile in 0.08% aqueous TFA (pH 2) for 60 min at a 25 ml/min flow rate. The purity (>99%) of the peptide was verified on a Nucleosil 5 μm C18 300 Å analytical column, using a 5–40% linear gradient of acetonitrile in 0.08% aqueous TFA (pH 2) for 20 min at a 1 ml/min flow rate (119 mg, yield 63%). Positive ion electrospray ionization mass spectrometry revealed a molecular mass of 1933.76 ± 0.54 (expected: 1934.26).

2.1.2. Fragment 9–38. Synthesis was performed using the extended double coupling protocol. Deblock steps were improved with two successive deliveries of piperidine instead of a single one (yield 84%). The Cys-16 residue of the sequence was substituted with a serine to avoid oligomerization effects. The cleavage method was the same as for fragment 25–38 except for peptide isolation, which was mostly improved by extraction of the Et_2O layer with water (182 mg, yield 61%). Crude product was purified according the latter method, on a Nucleoprep 20 μm C4 300 Å preparative column, using a 55–85% linear gradient of acetonitrile with 30% 2-propanol, in 0.08% aqueous TFA (pH 2) for 100 min at a 25 ml/min flow rate. During the purification steps, mass spectrometry revealed the presence of a contaminant with molecular mass of 3473.14, likely corresponding to a des-Ala product, scarcely resolvable by HPLC. In this case, five purification steps were necessary to remove this contaminant and to obtain with a low yield the target peptide. Purity (>95%) was finally verified on a Nucleosil 5 μm C4 300 Å analytical column, using a 52–65% linear gradient of acetonitrile in 0.08% aqueous TFA (pH 2) for 20 min at a 1 ml/min flow rate (11 mg, yield 6%). Positive ion electrospray ionization mass spectrometry revealed a molecular mass of 3544.20 ± 0.32 (expected: 3544.33).

2.2. NMR experiments

2.2.1. Fragment 9–38. Samples were prepared using 3 mM of the PMP1 fragment solubilized in 90:10 H_2O:D_2O solutions containing 120 mM of DPC-d_{38} micelles (CIL, USA). The pH value was adjusted to 5. ^{1}H-NMR experiments were carried out on a DRX 600 Bruker spectrometer at 35 and 45°C. Total correlated spectroscopy (TOCSY) and nuclear Overhauser enhancement spectroscopy (NOESY) spectra were recorded with mixing times of 80 ms and 100–250 ms respectively.

2.2.2. Fragment 25–38. Samples were prepared using 4 mM of the PMP1 fragment solubilized in 90:10 H_2O:D_2O solutions in the absence and presence of 120 mM of DPC-d_{38} micelles. The pH value was adjusted to 5. ^{1}H-NMR experiments were carried out on a DRX 500 Bruker spectrometer at 25 and 35°C. TOCSY and NOESY spectra were recorded with mixing times of 80 ms and 50–100 ms respectively. DPC titration experiments were performed by adding small aliquots of a 800 mM DPC stock solution to the peptide sample previously solubilized in a 90:10 H_2O:D_2O buffer. For modeling the Y25–F38 peptide, we used the latest release, 6.6, of Sybyl (Tripos Inc.). Tripos force field with electrostatics was used for minimization and dynamics.

3. Results

3.1. Conformation of the F9–F38 fragment in DPC micelles

Proton assignment of the F9–F38 fragment solubilized in perdeuterated DPC-d_{38} micelles was achieved using standard TOCSY and NOESY experiments. Fig. 1 shows the amide proton region of a NOESY spectrum, whose dispersion is characteristic of highly structured peptides. Fig. 2A summarizes the sequential and medium range NOEs involving the backbone protons. A set of intense NH–NH (*i*,*i*+1) NOEs associated with a continuous network of CαH–NH (*i*,*i*+3) and (*i*,*i*+4) contacts indicates the formation of a unique helix from the N-terminus up to Q32. The secondary structure of the F9–F38 peptide thus confirms that previously observed for the shorter A18–F38 peptide [10]. However, the residual NH signals observed in a D_2O solution for the F9–F38 peptide (Fig. 2A) arise from 11 consecutive residues (I17–K27) instead of only four in the case of the A18–F38 peptide [10]. This result assesses the stability gain provided by the additional helix turns.

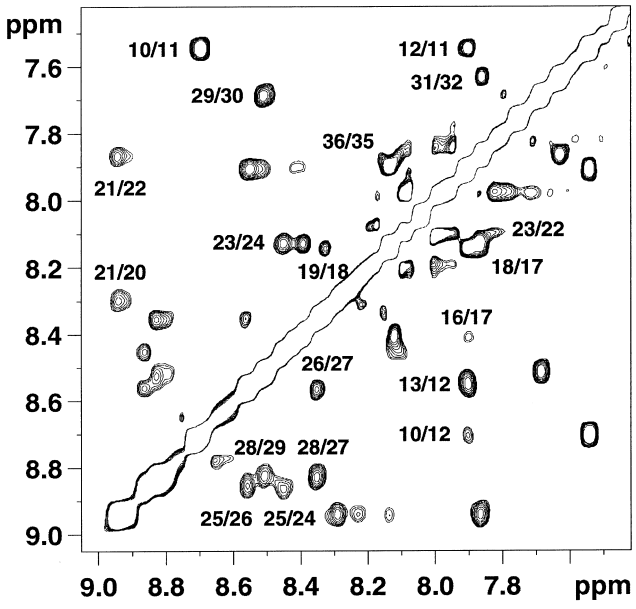

Fig. 1. Amide proton region of a NOESY spectrum (100 ms mixing time) of the F9–F38 peptide (3 mM) solubilized in the presence of DPC micelles (120 mM) in a H_2O:D_2O 9:1 solution pH 5 at 35°C.

The distribution of the residual NH signals along the I17–K27 segment also means that the residues of two helix turns (F9–S16) in the N-terminus but of only one helix turn (W28–Q32) in the C-terminus are less stable than those of the helix core. The difference in flexibility observed between the N- and C-termini can be readily explained as follows. First, the C-terminal part of the helix comprises the interfacial anchoring residues Y25 and W28, which contribute to its stability as compared to the N-terminus whose fraying is not restricted. Second, as mentioned in our paper dealing with the structure of the 18–38 fragment previously studied [10], the helix C-terminus of PMP1 is further stabilized by capping interactions, not observed in the N-terminus.

Examination of the Hα chemical shift indices (ΔδHα) of the F9–F38 peptide (gray bars in Fig. 3) highlights two important conformational features. First, they confirm the existence of a unique helix [16]. Second, in the C-terminus region extending from Q32 up to F38, the ΔδHα profile of the F9–F38 peptide fully fits that previously obtained for the A18–F38 peptide [10]. This result indicates that the average conformation of the cytoplasmic loop is similar for both peptides. In summary, the A18–F38 and F9–F38 fragments exhibit the same structural features, apart from the stability gain observed for the F9–F38 peptide, provided by the three additional helix turns.

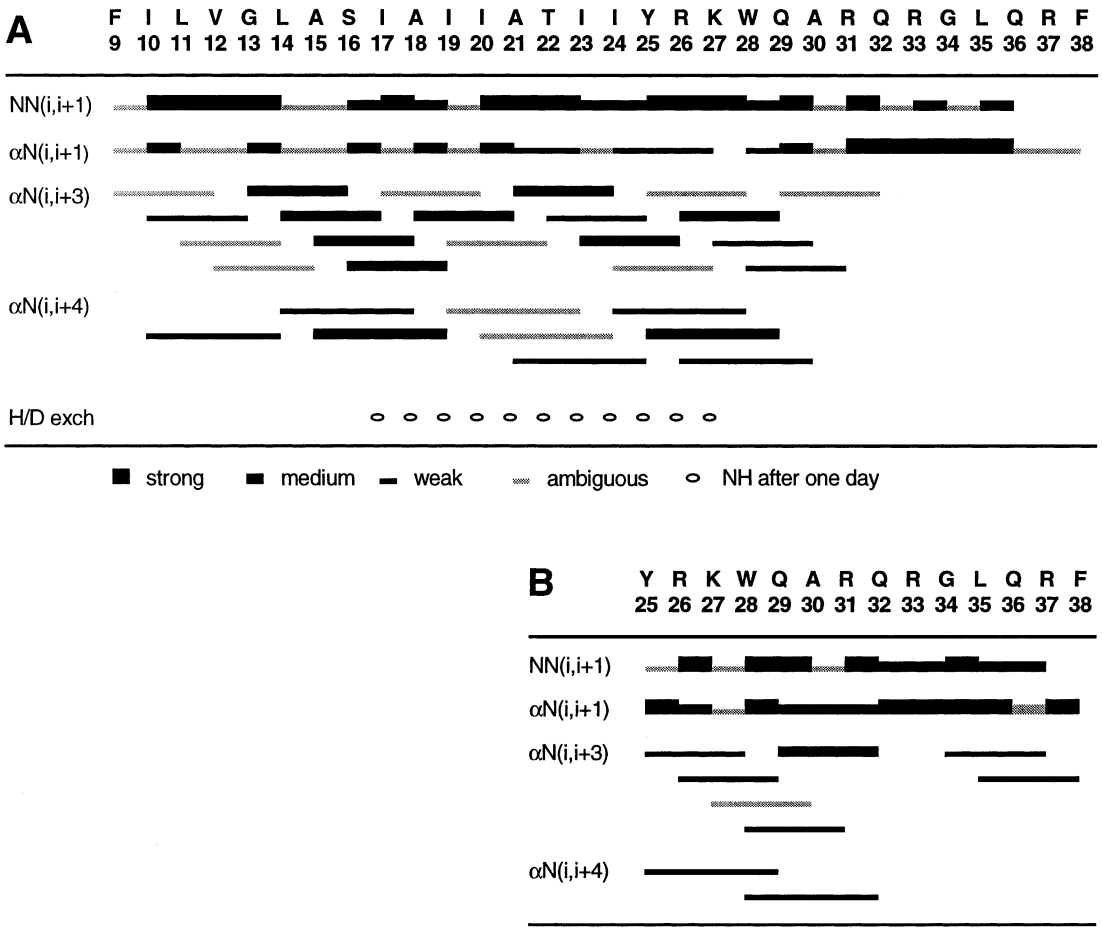

Fig. 2. Sequential and medium range NOEs involving the backbone protons of (A) the F9–F38 peptide and (B) the isolated cytoplasmic domain Y25–F38, solubilized in the presence of perdeuterated DPC micelles at 35°C, pH 5.0. The bar thickness refers to the NOE intensity (strong, medium, weak); a gray bar corresponds to an ambiguous NOE. The open symbol (H/D exch) indicates the residues of the F9–F38 peptide whose NH signal is still detected after 24 h in D_2O solution.

3.2. *Conformation of the Y25–F38 C-terminal domain in aqueous solution, in the absence and presence of DPC micelles*

In contrast with the previous PMP1 fragments studied, the isolated Y25–F38 C-terminal domain is soluble in pure aqueous solution. Fig. 4A shows the low-field region of the corresponding NMR spectrum. The very weak dispersion observed for the NH signals, around a mean value of 8.3 ppm, is characteristic of a highly disordered peptide. In the presence of a DPC concentration similar to that used for the F9–F38 peptide (120 mM), the spectral dispersion of the NH resonances dramatically increases (Fig. 4B), which reveals a marked structuring effect induced by the membrane-like environment. From TOCSY and NOESY spectra, proton assignment of the peptide solubilized in micelles was straightforward.

In a second step, the Y25–F38 C-terminal domain was titrated with DPC and the formation of its secondary structure was monitored following the Hα resonances. Fig. 5 presents the DPC dependence of selected Hα signals. Upon addition of DPC micelles, most of the Hα resonances undergo a high-field shift, characteristic of helical folds. The resulting titration curves exhibit similar sigmoid behaviors with a plateau region reached for a DPC concentration of 100 mM (Fig. 5). This is in particular the case for the two extreme residues, Y25 and F38, which suggests that the micelle interface exerts a cooperative structuring effect on the whole peptide. It has to be pointed out that the Hα signals of G34 and L35 are poorly sensitive to the DPC effect although a sigmoid transition can be detected in both cases.

Fig. 2B summarizes the NOE network connecting the backbone protons of the Y25–F38 C-terminal domain, solubilized

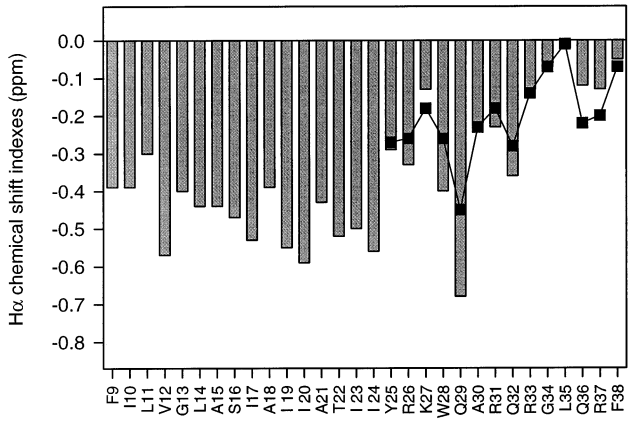

Fig. 3. ΔδHα chemical shift indices of (A) the F9–F38 peptide (gray bars) and (B) the isolated Y25–F38 C-terminal domain (black symbols) solubilized in the presence of perdeuterated DPC micelles at 35°C, pH 5.0.

in 120 mM DPC micelles. Remarkably, this small peptide exhibits a continuous set of αN(*i*,*i*+3) and αN(*i*,*i*+4) NOEs in the Y25–Q32 segment corresponding to the C-terminal part of the α-helix of the longer A18–F38 [10] and F9–F38 (Fig. 2A) peptides. In addition, one can observe two (*i*,*i*+3) NOEs, αN(34,37) and αN(35,38), which are absent in the NOESY spectra of the A18–F38 [10] and F9–F38 (Fig. 2A) peptides.

In Fig. 3, the ΔδHα indices of the Y25–F38 C-terminal domain (black symbols) are superimposed on those of the corresponding residues of the F9–F38 peptide (gray bars). The ΔδHα profile obtained for the isolated cytoplasmic domain is mostly close to that drawn by the corresponding residues of the F9–F38 peptide, except for two couples of residues, W28–Q29 on the one hand and Q36–R37 on the other hand. With regard to the Q36–R37 couple, their ΔδHα values are found to be significantly greater for the Y25–F38 peptide. This result can be readily related to the presence of the singular αN(34,37) and αN(35,38) NOEs previously mentioned and absent in the F9–F38 NOESY spectra. Besides, the preceding G34–L35 couple exhibits weak ΔδHα values in agreement with their poor dependence on the DPC concentration. Therefore, the NOE network (Fig. 2B) combined with the ΔδHα data (Fig. 3) of the Y25–F38 peptide delineate two distinct regions: (i) the Y25–Q32 segment that folds into a native regular α-helix and (ii) the C-terminal G34–F38 segment that adopts a non-native conformation which may be either a fraying α-helix turn or a short 3_{10}-helix, since no αN(*i*,*i*+4) NOE is observed between G34 and F38. Nevertheless, molecular modeling analysis using NOE data as constraints indicates that the 3_{10} conformation is mostly formed.

In the case of the W28–Q29 couple, the ΔδHα values found for the Y25–F38 peptide are significantly smaller than those obtained for the F9–F38 peptide. This decrease most probably results from an averaging of the ring current effect exerted by Y25 on the following *i*+3 and *i*+4 residues of the helix turn. In the isolated cytoplasmic domain, Y25 is the N-terminal residue and its side chain is certainly much more flexible than within the helix of the F9–F38 peptide.

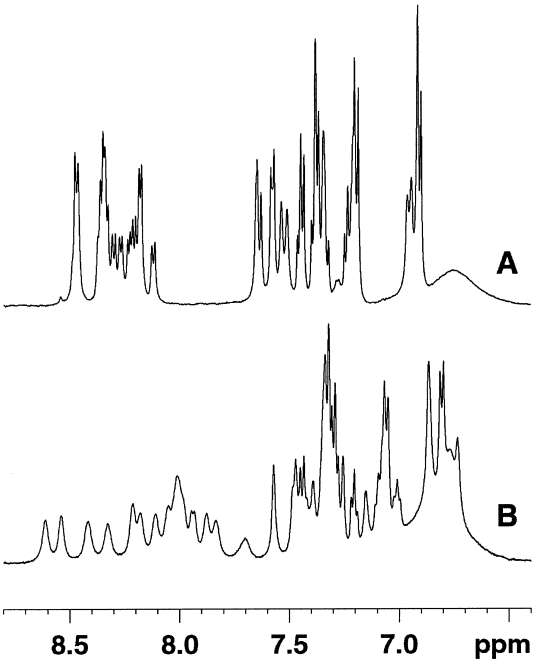

Fig. 4. Low-field region of the ^{1}H-NMR spectrum of the isolated Y25–F38 C-terminal domain in the absence (A) and presence (B) of perdeuterated DPC micelles, at 35°C, pH 5.0.

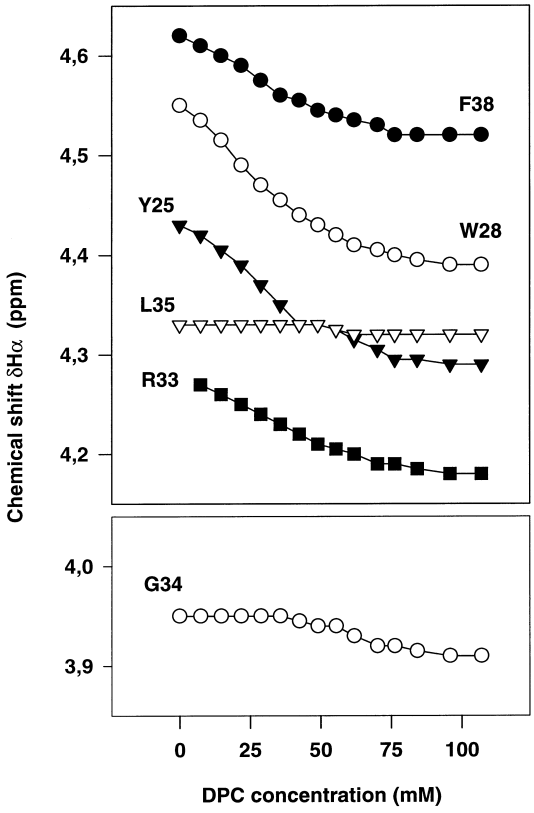

Fig. 5. DPC dependence of the Hα signal of residues Y25, W28, R33, G34, L35 and F38 of the isolated Y25–F38 C-terminal domain.

4. Discussion

A main point to be discussed is the coexistence of native and non-native conformations displayed by the Y25–F38 C-terminal domain. In the case of the A18–F38 [10] and F9–F38 (this work) peptides, the cytoplasmic domain is coupled to a hydrophobic span within the same helix structure, extending from the N-terminus up to Q32. The Y25–Q32 C-terminal segment of the helix thus points toward a direction perpendicular to the micelle surface and the following G34–F38 residues form a loop that folds back toward the hydrophobic interior of the micelle [10,11]. The 'snorkeling' ability of the basic side chains R26 and K27, associated with the anchoring interfacial property of Y25 and W28, ensures the appropriate positioning of the Y25–Q32 segment [10]. As a matter of fact, the Y_{25}-R-K-W_{28} motif constitutes a paradigm sequence since it contains all the four amino acids now identified as the key residues in the conformational features of membrane proteins at the interface [1,17,18].

In the case of the isolated Y25–F38 C-terminal domain, the Y25–Q32 segment still forms an α-helix in the presence of a membrane-like interface. Uncoupled from a hydrophobic stretch, the stable orientation of this amphipathic two-turn helix is obviously to lie parallel to the micelle surface. The persistence of G34 as a transition residue and the presence of

a short 3_{10}-helix in the C-terminal part can then be simply explained as follows. As the N-terminal region, the L_{35}-Q_{36}-R_{37}-F_{38} C-terminal segment exhibits an amphipathic sequence able to form a helical structure lying at a water–membrane interface. However, simple modeling considerations show that a full helix extending from Y25 up to F38 would expose F38 on the same side as that formed by the basic residues. In contrast, the occurrence of a break around the G34 residue followed by the formation of a short 3_{10}-helix allows the whole Y25–F38 sequence to adopt a regular amphipathic rod-like structure, in which the four hydrophobic residues Y25, W28, L35 and F38 are located on the same side, i.e. buried toward the micelle interior.

Therefore, in both the isolated Y25–F38 C-terminal domain and the longer PMP1 fragments, G34 plays its role of transition residue due to its well-known ability to adopt unusual ϕ,ψ values. However, the coupling with a hydrophobic anchor is necessary to drive the intrinsic conformational propensity of the cytoplasmic domain towards the appropriate interfacial fold. Comparing the A18–F38 and F9–F38 fragments shows that two hydrophobic helix turns, i.e. the A18–I24 segment, are sufficient. Adding supplementary helix turns in the N-terminal part of the hydrophobic span improves the secondary structure stability but does not exert any additional influence on the conformational features of the cytoplasmic domain. Our study thus shows that, in appropriate cases, relatively easy chemical synthesis of short protein fragments, i.e. such as the 18–38 peptide, may be suitable for investigating membrane protein folding. In contrast, the study of fully isolated extracellular/cytoplasmic domains may provide misleading interpretations. Nevertheless, we cannot rule out the possibility that the conformation obtained for the uncoupled PMP1 cytoplasmic domain has a biological relevance. When interacting with the ^{1}H-ATPase in the yeast plasma membrane, PMP1 may adopt a conformation different from that observed for the 18–38 and 9–38 fragments in a membrane-like environment.

References

[1] White, S. and Wimley, W.C. (1999) Annu. Rev. Biophys. Biomol. Struct. 28, 319–365.
[2] Bowie, J.U. (2000) Curr. Opin. Struct. Biol. 10, 435–437.
[3] MacKenzie, K.R., Prestegard, J.H. and Engelman, D.M. (1997) Science 276, 131–133.
[4] Kutateladze, T. and Overduin, M. (2001) Science 291, 1793–1796.
[5] Arora, A., Abildgaard, F., Bushweller, J.H. and Tamm, L.K. (2001) Nature Struct. Biol. 8, 334–338.
[6] Giragossian, C. and Mierke, D.F. (2001) Biochemistry 40, 3804–3809.
[7] Song, M., Shao, H., Mujeeb, A., James, T.L. and Miller, W.L. (2001) Biochem. J. 356, 151–158.
[8] Navarre, C., Ghislain, M., Leterme, S., Ferroud, C., Dufour, J.P. and Goffeau, A. (1992) J. Biol. Chem. 267, 6425–6428.
[9] Navarre, C., Catty, P., Leterme, S., Dietrich, F. and Goffeau, A. (1994) J. Biol. Chem. 269, 21262–21268.
[10] Beswick, V., Roux, M., Navarre, C., Coïc, Y.M., Huynh-Dinh, T., Goffeau, A., Sanson, A. and Neumann, J.M. (1998) Biochimie 80, 451–459.
[11] Beswick, V., Guerois, R., Ochsenbein, F., Coïc, Y.M., Huynh-Dinh, T., Tostain, J., Noël, J.P., Sanson, A. and Neumann, J.M. (1998) Eur. Biophys. J. 28, 48–58.
[12] Roux, M., Beswick, V., Coïc, Y.M., Huynh-Dinh, T., Sanson, A. and Neumann, J.M. (2000) Biophys. J. 79, 2624–2631.
[13] Carpino, L.A. and Han, G.Y. (1972) J. Org. Chem. 37, 3404–3409.
[14] Atherton, E., Fox, H., Harkiss, D. and Sheppard, R.C. (1978) J. Chem. Soc. Chem. Commun. 76, 539–540.
[15] Chang, C.D. and Meienhofer, J. (1978) Int. J. Peptide Protein Res. 11, 246–249.
[16] Wishart, D.S., Sykes, B.D. and Richards, F.M. (1991) J. Mol. Biol. 222, 311–333.
[17] Yuen, C.T.K., Davidson, A.R. and Deber, C.M. (2000) Biochemistry 39, 16155–16162.
[18] Killian, J.A. and von Heijne, G. (2001) Trends Biochem. Sci. 25, 429–434.